

Optical sideband selection in Optical IQ modulators driven by RF tones

AMENABAR Núria, MOLINA Maria, and TORRES Mireia
Universitat Politècnica de Catalunya, Enginyeria Física

(Dated: June 19, 2020)

This paper deals with IQ modulation using the nested Mach-Zehnder modulator, studying its different parameters and the effect of their value in the resulting signal. The main goal is to obtain the parameters for which a frequency shift is obtained, using different approaches. First, the Bessel functions are used to study the transfer function analytically. Then, numerical representations (both using the Bessel functions and Fourier coefficients) are plotted in order to further illustrate the results obtained, adding up with the spectra of some cases obtained using VPIphotonics, creating a full picture of the solution proposed.

I. INTRODUCTION

The photonic IQ modulator is a very versatile device which has recently become popular for a variety of uses. The activities within this project will aim at unveiling the potential of this kind of devices for applications in the radiofrequency domain such a wireless communications and remote sensing. The main objective will be to study the mathematical basis behind the nested Mach Zehnder Modulator, and then be able to use this tool to create a frequency shift to an input laser, observing its spectrum.

The frequency shifting is implemented applying optical carrier suppression and single-sideband modulation using a nested Mach-Zahnder interferometer.

II. DEVICE DESCRIPTION

A Mach-Zehnder IQ modulator (MZM) uses the Pockels effect to create a phase shift between the two branches in which the light input beam has been split, and then makes them interfere, modulating that way the amplitude and the phase.

The Pockels effect consists in inducing a change in the refractive index of each arm, which depends on the electric voltage applied in each electrode. Changing the refractive index, the propagation velocity of the light changes. That way, the phase difference between the two branches is created.

The transfer function of a single MZM is:

$$E_{out} = E_{in} \left((1 - \alpha) e^{-j \frac{\pi}{V_{\pi 1}} V_1} + \alpha e^{-j \frac{\pi}{V_{\pi 2}} V_2} \right) \quad (1)$$

Where V_1 and V_2 are the voltages applied to each branch. $V_{\pi 1}$ and $V_{\pi 2}$ are specifications of the engine, the voltage required to produce a phase shift of π . In the following simulations this parameter is set as 1 for simplicity. α is the interferometric splitting ratio, in the ideal case it is 0.5.

One of the most used configurations for a MZM and the one which will be used in this paper is the push-pull configuration, where $V_1 = -V_2$. It increases the relative phase shift in one path and decreases it in the other path, with the same magnitude.

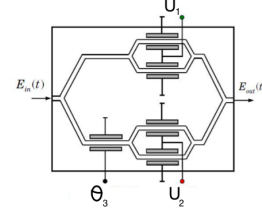


FIG. 1. Nested Mach Zehnder modulator

A nested Mach-Zehnder modulator consists in two main branches, with a voltage difference between them, and one MZM in each branch. The incoming beam is split into the two main branches, where the first phase change is done due to the difference of voltage applied. After that, the each MZM modulates the beam in the corresponding branch. Lastly, both outputs are joined, interfering with each other and resulting in the modulated signal.

The transfer function of the last apparatus is described by:

$$E_{nMZM} = \frac{E_{in}}{2} \left(\cos \frac{\pi}{2V_{\pi}} U_1 + e^{i\theta_3} \cos \frac{\pi}{2V_{\pi}} U_2 \right) \quad (2)$$

Where θ_3 is the voltage difference between the two main branches, and U_1 and U_2 are the voltages applied to the MZM in each branch. It should be noted that each voltage has a bias component, and a small signal component.

To simplify notation, the following parameters are defined for $i = 1, 2$:

$$\frac{\pi}{2V_{\pi}} U_i = \frac{\pi}{2V_{\pi}} V_{bias_i} + V_{RF_i} = \frac{\theta_i}{2} + \frac{m_i}{2} \cos(\omega_{RF} t)$$

Therefore, equation (2) reads:

$$E_{out} = \cos \left(\frac{\theta_1}{2} + \frac{m_1}{2} \cos \omega t \right) + e^{j\theta_3} \cos \left(\frac{\theta_2}{2} + \frac{m_2}{2} \cos \omega t + \varphi \right) \quad (3)$$

III. FREQUENCY SHIFTING

Frequency shifting is achieved by modifying the signal spectrum so that the band associated to the carrier frequency and one of the first side bands are null and the other first band has a magnitude different from zero.

The trivial values of the different parameters used to achieve this are: $\theta_1 = \theta_2 = \pi$, $\theta_3 = \varphi = \frac{\pi}{2}$. However, when working on the laboratory the voltage can be set to different values, which changes the phase difference φ and thus, the configuration no longer shifts the frequency.

To achieve a frequency shifting for the different values of φ different approaches have been used, all of them taking as a variable the parameters θ_3 and φ and setting $\theta_1 = \theta_2 = \pi$.

It should be remarked that only the trivial values set the carrier and one of the first bands to zero. However, setting a relative magnitude between them could shift the frequency under the desired accuracy. Illustrating for which φ it will be possible to do a frequency shift for different relative magnitudes is one of the go??

IV. ANALYTICAL APPROACH

In order to understand the effect of the nMZM, the modulator's transfer function has been developed to obtain the amplitudes of the harmonics. Looking at these amplitudes it can be seen which side bands, or harmonics signals, are canceled when the laser passes through the device, and what happens with the carrier band.

The analytical equation of the amplitude of each band is calculated using the Bessel functions and it is shown below. The procedure to obtain them is explained in Appendix 1.

This report is based in the small signal approximation and thus, the third or larger side bands are despicable. That is why their equation will not be used here. Due to this approximation, the m parameter (amplitude of the voltage signal) has to be a small number.

Carrier Band:

$$A_0 = J_0\left(\frac{m}{2}\right) \cdot \left(\cos\left(\frac{\theta_1}{2}\right) + e^{i\theta_3} \cos\left(\frac{\theta_2}{2}\right)\right)$$

First positive side Band:

$$A_1 = J_1\left(\frac{m}{2}\right) \cdot \left(\sin\left(\frac{\theta_1}{2}\right) + e^{i(\theta_3+\varphi)} \sin\left(\frac{\theta_2}{2}\right)\right)$$

First negative side band:

$$A_{-1} = J_1\left(\frac{m}{2}\right) \cdot \left(\sin\left(\frac{\theta_1}{2}\right) + e^{i(\theta_3-\varphi)} \sin\left(\frac{\theta_2}{2}\right)\right)$$

Second positive side band:

$$A_2 = J_2\left(\frac{m}{2}\right) \cdot \left(\cos\left(\frac{\theta_1}{2}\right) + e^{i(\theta_3+2\varphi)} \cos\left(\frac{\theta_2}{2}\right)\right)$$

Second negative side band:

$$A_{-2} = J_2\left(\frac{m}{2}\right) \cdot \left(\cos\left(\frac{\theta_1}{2}\right) + e^{i(\theta_3-2\varphi)} \cos\left(\frac{\theta_2}{2}\right)\right)$$

$J\left(\frac{m}{2}\right)$ is the Bessel function of the amplitude of the voltage signal applied to the small MZM's.

As explained in the previous section, depending on the configuration of the modulator, the bias voltage applied to each of the small MZM (θ_1 , θ_2), its phase difference φ and the phase difference due to the voltage applied in one of the branches θ_3 , different results are obtained.

If the bias voltage is set to the null point ($\theta_1 = \theta_2 = \pi$), the even and the carrier bands cancel out. If it is set to the quadrature point ($\theta_1 = \theta_2 = \frac{\pi}{2}$), the odd bands cancel and just the carrier and the first bands remain. This is due to the sinusoidal characteristics of the equations. This is the reason why, when the parameters for frequency shifting are chosen, θ_1 and θ_2 are set to the null point. Varying the θ_3 parameter, the interference between the waves coming from the two small MZM interfere differently, and can cancel bands even when the bias voltage θ_1 and θ_2 are not in the quadrature or null points.

Finally, φ is the parameter that makes the spectrum asymmetric for positive and negative bands. As it can be seen in the equations, for positive bands, this value is added to θ_3 inside the exponential and for negative bands it is subtracted. Due to this property of the nested MZM, frequency shift can be produced.

Despite of this, frequency shifting does not happen for any value of θ_3 and φ . The trivial configuration, the most used in laboratories, is explained in the previous section. Using the expressions of the complex amplitude of the side bands, other possible values of θ_3 and φ that accomplish frequency shift have been found. In table I, examples of these parameters are shown:

θ_3	90°	92°	94°	99°	105°	110°
φ	90°	87°	85°	81°	74°	69°

TABLE I. Frequency shifting for $\theta_1 = \theta_2 = \pi$ and diferents θ_3 and φ .

V. MATLAB SIMULATION

The main goal of this section is to illustrate how the frequency bands change with the different parameters of

the nMZM. In order to do this the codes in the Appendix have been used. The Fourier coefficients are calculated and represented to see at which values the frequency shift is achieved and, moreover, to confirm the accuracy of the analytical results found in the previous section.

Starting from equation (3), the complex Fourier coefficients can be calculated.

Their amplitude describe the frequency bands, which depend on the magnitude of the different parameters. Throughout the following discussion, the values of θ_1 , θ_2 , m_1 and m_2 are taken as constants of values π , π , 0.2 and 0.2. On the other hand, due to the reason stated on the Frequency Shifting section, θ_3 and φ are set to be the variables.

Figure 2 includes three plots of the carrier band and the first negative and positive bands for different values of ϕ and θ_3 .

The black regions on the graph show those combinations of the variables which fulfill the condition for the frequency shift to be achieved: a difference of 20 dB between the carrier and the first positive band with respect to the first positive side band.

As it can be seen the carrier band is almost null for all the values, this is due to the fact that θ_1 and θ_2 are both π .

Figure 3 is a representation of the amplitude of the first bands for different values of θ_3 for fixed values of φ . It can be seen that, defining $\delta\theta = \theta_3 - \pi$ the magnitude of the positive band for $\theta_3 = \pi + \delta\theta$ and the value of the negative band for $\theta_3 = \pi - \delta\theta$ is the same. Furthermore, for larger values of φ the value of θ_3 for which the negative and positive first bands are null increases its distance with respect to π .

It can be observed that the only value for which the frequency shift is achieved with one of the bands set to a null value is for $\phi = 90^\circ$, while for other values of this parameter a relative magnitude criterion should be used.

Figure 4 represents the values of the variables which can be used to obtain a frequency shift for different conditions. The z axis represents the difference in dB between the first negative band and the other ones. It can be seen that when a higher precision is imposed, less combinations of variables fulfill it. It is important to take this result into consideration when determined accuracy is required.

VI. VPIPHOTONICS SIMULATION

After all the analysis, optical spectrums of the main cases can be found in this section. Spectrums have been made using VPIphotonics, a simulation software for photonic design automation, using a program that resembled a nMZM.

The optical spectrum corresponding to frequency shifting can be seen in FIG 5. The values used to obtain it are $m_1 = m_2 = 0.2$, $\theta_1 = \theta_2 = \pi$ and $\theta_3 = \phi = \pi/2$. The exact same spectrum can be obtained without vary-

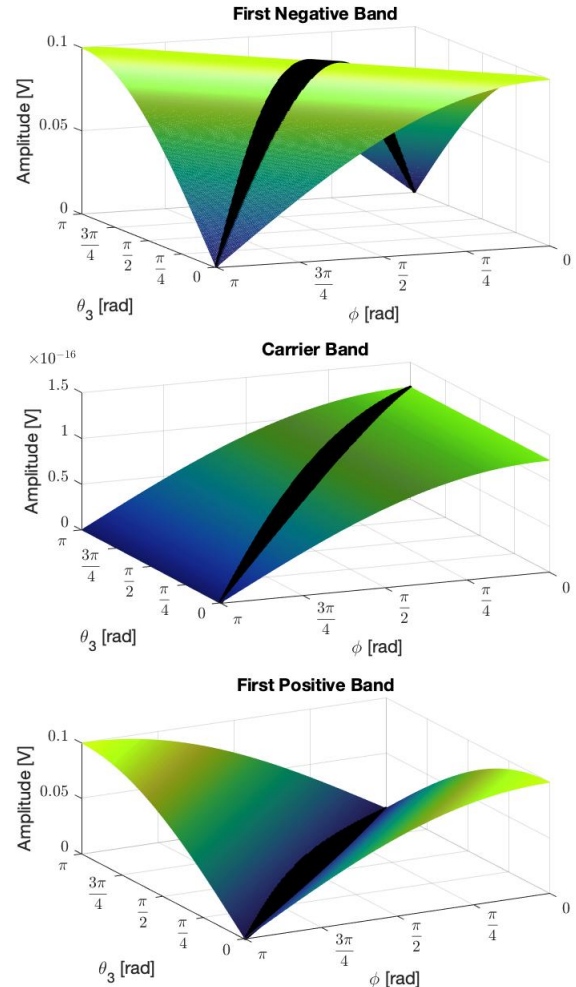


FIG. 2. Plot of the frequency bands with $\theta_1 = \pi$, $\theta_2 = \pi$, $m_1 = 0.2$, $m_2 = 0.2$.

ing θ_1 , θ_2 , m_1 or m_2 , using some determinate values of θ_3 and ϕ (the ones seen in table 1).

The value of both m can variate and continue obtaining the same peaks with different amplitude (higher values of m increase the power of the peak). But, the problem that must be taken into account that the increase of the power also affects to other peaks (second, third harmonics...) that for frequency shifting need to be irrelevant with respect to the main one. To sum up, value of m has to be chosen carefully so that the power of the main band is good, but so that we can still despise other peaks.

Another interesting aspect to comment is the sign of the frequency shift: by changing the sign of either ϕ or θ_3 , instead of getting the peak at -1, it will be obtained in +1.

Frequency multiplying is another possible application of the nMZM: Obtaining a multiple harmonic from the

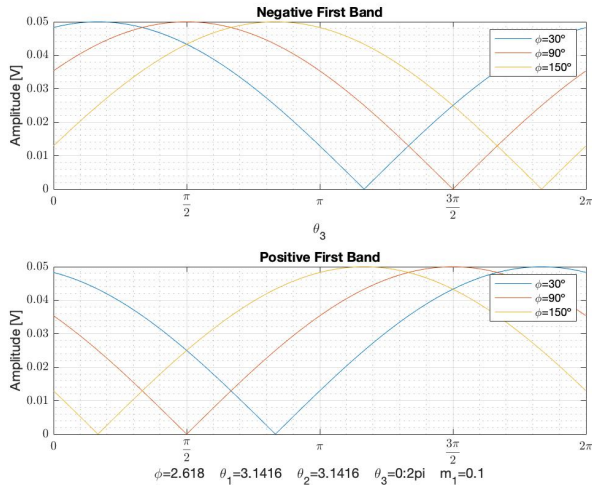


FIG. 3. Plot of the amplitude of the first positive and negative bands for $\phi = 30^\circ, 90^\circ, 150^\circ$ and for θ_3 from 0 to 2π

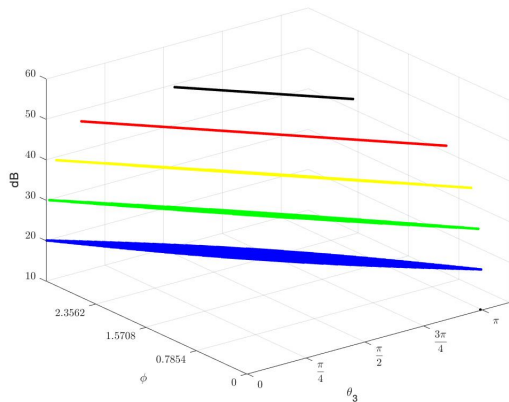


FIG. 4. Plot of the values of θ_3 and φ which fulfill an amplitude difference of different dB, written in the y axis

input one. In this case, using the parameters $\theta_1 = \theta_2 = 0$ (no bias component in the small MZM), $\theta_3 = \pi$, $\phi = 90$ and $m_1 = m_2 = 1.22$. Notice that the values of m are chosen to be, multiplied by two, the first zero of the Bessel functions (2.44), to that way cancel the main carrier. The second band is also zero because of the electric phase shift, which creates asymmetry. This leaves the third band (at ± 2).

As stated before, m can be modified in small quantities to get approximately the same spectrum with different amplitude.

The resulting spectrum can be seen in FIG 6, where the third bands are the only significant ones.

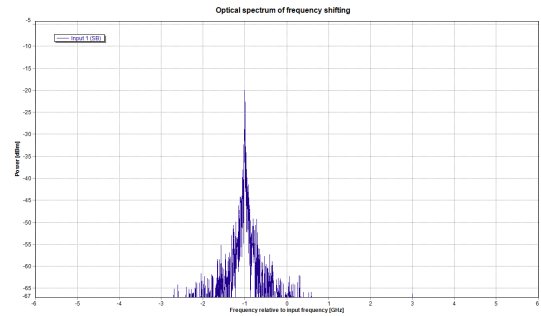


FIG. 5. Frequency shifting simulation (VPI)

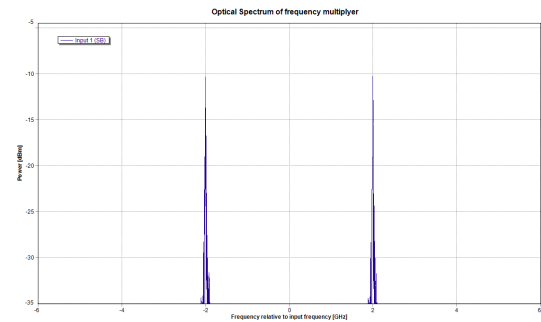


FIG. 6. Frequency multiplier simulation (VPI)

VII. CONCLUSIONS

In this paper, the properties and the operation of the nested Mach-Zehnder modulator have been studied. It has been done analytically, with Bessel functions, and numerically analyzing the spectrum of the transfer function of the device for different parameters.

Also, another possible values for $\theta_1, \theta_2, \theta_3$ and φ that accomplish the frequency shifting have been discovered. This is an important application because its configuration is not always possible to do. So, with these results, it is expected to be able to reach the same objective without being forced to make the same set-up settling always the parameters to the trivial ones.

[1] M. Masanas, S. Cichy, Full duplex network access with colorless and source-free optical network units. Universitat Politècnica de Catalunya, 2019.
 [2] H. Chena, J. Wanga, H. Lua, T. Ningb, L. Peib, J. Lib, Study on millimeter-wave photonic generator scheme with tunable multiplication factors. Optik - International Journal for Light and Electron Optics 202 (2020).

[3] Coherent Optical Systems: https://www.photonics.ntua.gr/OptikaDiktya_Epikoinwnias/Lecture.4.CoherentOptical_DSP.pdf
 [4] F. A. Gutierrez, P. Perry, F. Smith, A. D. Ellis, L. P. Barry, Optimum Bias Point in Broadband Subcarrier Multiplexing With Optical IQ Modulators. Journal of Lightwave Technology, 2015, pages 258-265.

APPENDIX

Appendix 1: Analytical development

The transfer function of the nMZM modulator is the next one:

$$\frac{E_{out}}{E_{in}} = \frac{1}{2} \left[\cos \left(\frac{\theta_1 + m \cos(w_{RF}t)}{2} \right) + e^{i\theta_3} \cos \left(\frac{\theta_2 + m \cos(w_{RF}t + \varphi)}{2} \right) \right]$$

With $\theta_1 = \frac{V_{B1}}{V_{pi}} \pi$ and $\theta_2 = \frac{V_{B2}}{V_{pi}} \pi$.

Using Jacobi-Anger relations:

$$\begin{aligned} \cos(z \cos(\theta)) &= J_0(z) + \sum_{n=-\infty}^{-1} (-1)^n J_{2n}(z) e^{i2n\theta} + \sum_{n=1}^{\infty} (-1)^n J_{2n}(z) e^{i2n\theta} \\ \sin(z \cos(\theta)) &= - \sum_{n=-\infty}^{-1} (-1)^n J_{2n-1}(z) e^{i(2n-1)\theta} - \sum_{n=1}^{\infty} (-1)^n J_{2n-1}(z) e^{i(2n-1)\theta} \end{aligned}$$

The first term of the transfer function is written with Bessel functions in the following way:

$$\begin{aligned} \cos \left(\frac{\theta_1 + m \cos(w_{RF}t)}{2} \right) &= \cos \left(\frac{\theta_1}{2} \right) \cos \left(\frac{m \cos(w_{RF}t)}{2} \right) - \sin \left(\frac{\theta_1}{2} \right) \sin \left(\frac{m \cos(w_{RF}t)}{2} \right) = \\ &= \cos \left(\frac{\theta_1}{2} \right) \left(J_0 \left(\frac{m}{2} \right) + \sum_{n=1}^{\infty} (-1)^n J_{2n} \left(\frac{m}{2} \right) e^{-i2nw_{RF}t} + \sum_{n=1}^{\infty} (-1)^n J_{2n} \left(\frac{m}{2} \right) e^{i2nw_{RF}t} \right) - \sin \left(\frac{\theta_1}{2} \right) \cdot \\ &\quad \left(- \sum_{n=1}^{\infty} (-1)^n J_{2n-1} \left(\frac{m}{2} \right) e^{i(2n-1)w_{RF}t} - \sum_{n=1}^{\infty} (-1)^n J_{2n-1} \left(\frac{m}{2} \right) e^{-i(2n-1)w_{RF}t} \right) \end{aligned}$$

And the second term:

$$\begin{aligned} e^{i\theta_3} \cos \left(\frac{\theta_2 + m \cos(w_{RF}t + \varphi)}{2} \right) &= \\ e^{i\theta_3} \left(\cos \left(\frac{\theta_2}{2} \right) \cos \left(\frac{\cos(w_{RF}t + \varphi)}{2} \right) - \sin \left(\frac{\theta_2}{2} \right) \sin \left(\frac{\cos(w_{RF}t + \varphi)}{2} \right) \right) &= e^{i\theta_3} \cos \left(\frac{\theta_2}{2} \right) \cdot \\ \left(J_0 \left(\frac{m}{2} \right) + \sum_{n=1}^{\infty} (-1)^n J_{2n} \left(\frac{m}{2} \right) e^{-i2nw_{RF}t} e^{-i2n\varphi} + \sum_{n=1}^{\infty} (-1)^n J_{2n} \left(\frac{m}{2} \right) e^{i2nw_{RF}t} e^{i2n\varphi} \right) - e^{i\theta_3} \sin \left(\frac{\theta_2}{2} \right) \cdot \\ \left(- \sum_{n=1}^{\infty} (-1)^n J_{2n-1} \left(\frac{m}{2} \right) e^{i(2n-1)w_{RF}t} e^{i(2n-1)\varphi} - \sum_{n=1}^{\infty} (-1)^n J_{2n-1} \left(\frac{m}{2} \right) e^{-i(2n-1)w_{RF}t} e^{-i(2n-1)\varphi} \right) \end{aligned}$$

Finally, both terms are added:

$$\frac{E_{out}}{E_{in}} = \frac{1}{2} \left[J_0 \left(\frac{m}{2} \right) \cdot \left(\cos \left(\frac{\theta_1}{2} \right) + e^{i\theta_3} \cos \left(\frac{\theta_2}{2} \right) \right) - J_1 \left(\frac{m}{2} \right) \cdot \left(\sin \left(\frac{\theta_1}{2} \right) + e^{i(\theta_3 + \varphi)} \sin \left(\frac{\theta_2}{2} \right) \right) e^{iw_{RF}t} + \dots \right]$$

Appendix 2: Code to plot the frequency bands in 3D

```

1
2 %% Using Bessel functions
3 clear all
4 clc
5
6 Nwt=1e7; wt=linspace(-pi,pi,Nwt); dwt=2*pi/Nwt; t1=pi; t2=pi; m=0.2;
7 fs=[]; pas=0.01; t33=0:pas:pi; pee=0:pas:pi;
8
9 M0=zeros(length(t33),length(pee));
10 MA1=zeros(length(t33),length(pee));
11 MB1=zeros(length(t33),length(pee));
12
13 for pp=1:length(pee)
14     phi=pee(pp);
15     for tt=1:length(t33)
16
17         t3=t33(tt);
18
19         A0=abs(besselj(0,m/2)*(cos(t1/2)+exp(1i*t3)*cos(t2/2)));
20         A1=abs(besselj(1,m/2)*(sin(t1/2)+exp(1i*(t3+phi))*sin(t2/2)));
21         B1=abs(besselj(1,m/2)*(sin(t1/2)+exp(1i*(t3-phi))*sin(t2/2)));
22
23         M0(tt,pp)=A0; MA1(tt,pp)=A1; MB1(tt,pp)=B1;
24
25         if 20<20*log10(B1/A0) && 20<20*log10(B1/A1)
26             fs=[fs; t3 phi M0(tt,pp) MA1(tt,pp) MB1(tt,pp)];
27         end
28     end
29 end
30
31 subplot(3,1,1), mesh(t33,pee,MB1), title('First_Negative_Band'), hold on
32 for ii=1:length(fs)
33     plot3(fs(ii,2),fs(ii,1),fs(ii,5),'k. ')
34 end
35 xlabel('\theta_3'), ylabel('\phi'), l1 = light; l1.Position = [160 400 80];
36 l1.Style = 'local'; l1.Color = [0 0.8 0.8]; l2 = light;
37 l2.Position = [.5 -1 .4]; l2.Color = [0.8 0.8 0];
38
39 subplot(3,1,2), mesh(t33,pee,M0), hold on
40 for ii=1:length(fs)
41     plot3(fs(ii,2),fs(ii,1),fs(ii,3),'k. ')
42 end
43 l1 = light; l1.Position = [160 400 80]; l1.Style = 'local';
44 l1.Color = [0 0.8 0.8]; l2 = light; l2.Position = [.5 -1 .4];
45 l2.Color = [0.8 0.8 0]; s.FaceColor = [0.9 0.2 0.2];
46 title('Carrier_Band'), xlabel('\theta_3'), ylabel('\phi')
47
48 subplot(3,1,3), mesh(t33,pee,MA1), hold on
49 for ii=1:length(fs)
50     plot3(fs(ii,2),fs(ii,1),fs(ii,4),'k. ')
51 end
52 l1 = light; l1.Position = [160 400 80]; l1.Style = 'local';
53 l1.Color = [0 0.8 0.8]; l2 = light; l2.Position = [.5 -1 .4];
54 l2.Color = [0.8 0.8 0]; s.FaceColor = [0.9 0.2 0.2];
55 title('First_Positive_Band'), xlabel('\theta_3'), ylabel('\phi')
56
57 %% Using the fourier coefficients
58
59 clear all
60 clc
61
62 Nwt=1e5; wt=linspace(-pi,pi,Nwt); dwt=2*pi/Nwt; t1=pi; t2=pi;
63 m1=0.2; m2=0.2; fs=[]; pas=0.05;

```

```

64
65 t33=0:pas:pi; pee=0:pas:pi; M0=zeros(length(t33),length(pee));
66 MP1=zeros(length(t33),length(pee)); MN1=zeros(length(t33),length(pee));
67
68 for pp=1:length(pee)
69     pe=pee(pp);
70 for tt=1:length(t33)
71
72     t3=t33(tt);
73
74     Eout=cos(t1/2+m1/2*cos(wt))+exp(j*t3)*cos(t2/2+m2/2*cos(wt+pe));
75
76     c0=1/(2*pi)*sum(Eout)*dwt;
77     c_p1=1/(2*pi)*sum(Eout.*exp(-j*wt))*dwt;
78     c_n1=1/(2*pi)*sum(Eout.*exp(j*wt))*dwt;
79
80     m0=abs(c0); m_p1=abs(c_p1); m_n1=abs(c_n1);
81     M0(tt,pp)=m0; MP1(tt,pp)=m_p1; MN1(tt,pp)=m_n1;
82
83     if 20<20*log10(m_n1/m0) & 20<20*log10(m_n1/m_p1)
84         fs=[fs; pe t3 M0(tt,pp) MP1(tt,pp) MN1(tt,pp)];
85     end
86 end
87 end
88
89 figure(1)
90 subplot(1,3,1), mesh(t33,pee,MN1), hold on
91 for ii=1:length(fs)
92     plot3(fs(ii,2),fs(ii,1),fs(ii,5),'k. ')
93 end
94 l1 = light; l1.Position = [160 400 80]; l1.Style = 'local';
95 l1.Color = [0 0.8 0.8]; l2 = light; l2.Position = [.5 -1 .4];
96 l2.Color = [0.8 0.8 0]; title('1st_Negative_Band'),
97 xlabel('\theta_3'), ylabel('\phi')
98
99 subplot(1,3,2), mesh(t33,pee,M0), hold on
100 for ii=1:length(fs)
101     plot3(fs(ii,2),fs(ii,1),fs(ii,3),'k. ')
102 end
103 l1 = light; l1.Position = [160 400 80]; l1.Style = 'local';
104 l1.Color = [0 0.8 0.8]; l2 = light; l2.Position = [.5 -1 .4];
105 l2.Color = [0.8 0.8 0]; title('Carrier_Band'),
106 xlabel('\theta_3'), ylabel('\phi')
107
108 subplot(1,3,3), mesh(t33,pee,MP1), hold on
109 for ii=1:length(fs)
110     plot3(fs(ii,2),fs(ii,1),fs(ii,4),'k. ')
111 end
112 l1 = light; l1.Position = [160 400 80]; l1.Style = 'local';
113 l1.Color = [0 0.8 0.8]; l2 = light; l2.Position = [.5 -1 .4];
114 l2.Color = [0.8 0.8 0]; title('1st_Positive_Band'),
115 xlabel('\theta_3'), ylabel('\phi')

```


Appendix 3: Spectrum representation function

```

1 function iqouts = iqouts(pe, t1, t2, t3, m1, m2)
2
3 Nwt=1e7; wt=linspace(-pi, pi, Nwt); dwt=2*pi/Nwt;
4
5 Eout=cos(t1/2+m1/2*cos(wt))+exp(j*t3)*cos(t2/2+m2/2*cos(wt+pe));
6
7 c0=2/pi*sum(Eout)*dwt;
8
9 c_p1=1/(2*pi)*sum(Eout.*exp(-j*wt))*dwt;
10 c_n1=1/(2*pi)*sum(Eout.*exp(j*wt))*dwt;
11
12 c_p2=1/(2*pi)*sum(Eout.*exp(-2*j*wt))*dwt;
13 c_n2=1/(2*pi)*sum(Eout.*exp(2*j*wt))*dwt;
14
15 c_p3=1/(2*pi)*sum(Eout.*exp(-3*j*wt))*dwt;
16 c_n3=1/(2*pi)*sum(Eout.*exp(3*j*wt))*dwt;
17
18 c_p4=1/(2*pi)*sum(Eout.*exp(-4*j*wt))*dwt;
19 c_n4=1/(2*pi)*sum(Eout.*exp(4*j*wt))*dwt;
20
21 c_p5=1/(2*pi)*sum(Eout.*exp(-5*j*wt))*dwt;
22 c_n5=1/(2*pi)*sum(Eout.*exp(5*j*wt))*dwt;
23
24 m0=abs(c0);
25
26 m_p1=abs(c_p1); m_n1=abs(c_n1);
27
28 m_p2=abs(c_p2); m_n2=abs(c_n2);
29
30 m_p3=abs(c_p3); m_n3=abs(c_n3);
31
32 m_p4=abs(c_p4); m_n4=abs(c_n4);
33
34 m_p5=abs(c_p5); m_n5=abs(c_n5);
35
36 pn = [-5 -4 -3 -2 -1 0 1 2 3 4 5];
37 m_pn = [m_n5 m_n4 m_n3 m_n2 m_n1 m0 m_p1 m_p2 m_p3 m_p4 m_p5];
38
39 pee=['\phi=', num2str(pe)];
40 t11=['\theta_1=', num2str(t1)];
41 t22=['\theta_2=', num2str(t2)];
42 t33=['\theta_3=', num2str(t3)];
43 m11=['m_1=', num2str(m1)];
44 m22=['m_2=', num2str(m2)];
45 info=[pee t11 t22 t33 m11 m22];
46
47 iqouts = stem(pn, m_pn)
48 xlabel(info)

```

Appendix 4: Frequency shifting plot for different conditions

```

1 clear all
2 clc
3
4 Nwt=1e7; wt=linspace(-pi,pi,Nwt); dwt=2*pi/Nwt; t1=pi; t2=pi; m=0.2;
5 fs=[]; pas=0.01; t33=0:pas:pi; pee=0:pas:pi; db=[];
6 MK=zeros(315,315);
7
8 M0=zeros(length(t33),length(pee));
9 MA1=zeros(length(t33),length(pee));
10 MB1=zeros(length(t33),length(pee));
11
12 for dbb=10:10:80
13     for pp=1:length(pee)
14         phi=pee(pp);
15         for tt=1:length(t33)
16
17             t3=t33(tt);
18
19             A0=abs(besselj(0,m/2)*(cos(t1/2)+exp(1i*t3)*cos(t2/2)));
20             A1=abs(besselj(1,m/2)*(sin(t1/2)+exp(1i*(t3+phi))*sin(t2/2)));
21             B1=abs(besselj(1,m/2)*(sin(t1/2)+exp(1i*(t3-phi))*sin(t2/2)));
22
23             M0(tt,pp)=A0; MA1(tt,pp)=A1; MB1(tt,pp)=B1;
24             MK(tt,pp)=dbb;
25
26             if dbb<20*log10(B1/A0) && dbb<20*log10(B1/A1)
27
28                 fs=[fs; t3 phi M0(tt,pp) MA1(tt,pp) MB1(tt,pp)];
29             end
30         end
31     end
32
33     C = {'k.', 'b.', 'g.', 'y.', 'r.', 'k.', 'b.', 'y.', 'r.', 'k.'};
34
35     figure(1)
36     for ii=1:length(fs)
37         plot3(fs(ii,2), fs(ii,1), dbb, C{(dbb-10)/10+1})
38     end
39     grid on
40     xlabel('\theta_3'), ylabel('\phi'), zlabel('dB')
41     l1 = light; l1.Position = [160 400 80];
42     l1.Style = 'local'; l1.Color = [0 0.8 0.8]; l2 = light;
43     l2.Position = [.5 -1 .4]; l2.Color = [0.8 0.8 0];
44     set(gca, 'xtick', [0:pi/4:pi])
45     set(gca, 'ytick', [0:pi/4:pi])
46     set(gca, 'TickLabelInterpreter', 'latex');
47     set(gca, 'XTickLabel', {'0', '$\frac{\pi}{4}$', '$\frac{\pi}{2}$', '$\frac{3\pi}{4}$', '$\pi$'},
48         'YTickLabel', {'0', '$\frac{\pi}{4}$', '$\frac{\pi}{2}$', '$\frac{3\pi}{4}$', '$\pi$'})
49     hold on
50     fs=[];
51     end

```

Appendix 5: Plot of the bands changing θ_3

```

1 clear all
2 clc
3
4
5 Nwt=1e7;
6 wt=linspace(-pi, pi, Nwt);
7 dwt=2*pi/Nwt;
8 t1=pi; t2=pi; m1=0.1; m=0.1; phi=20*2*pi/360;
9
10 banda0=[]; banda1neg=[]; banda1pos=[];
11 pt0banda0=[]; pt0banda1neg=[]; pt1banda1pos=[];
12 fs=[];
13 pas=0.01;
14
15 for phi=30*2*pi/360:60*2*pi/360:150*2*pi/360
16 for t3=0:pas:2*pi
17
18 A0=abs(besselj(0,m/2)*(cos(t1/2)+exp(1i*t3)*cos(t2/2)));
19 A1=abs(besselj(1,m/2)*(sin(t1/2)+exp(1i*(t3+phi))*sin(t2/2)));
20 B1=abs(besselj(1,m/2)*(sin(t1/2)+exp(1i*(t3-phi))*sin(t2/2)));
21 banda0=[banda0 A0];
22 banda1pos=[banda1pos A1];
23 banda1neg=[banda1neg B1];
24
25 end
26 pee=['\phi=', num2str(phi)]; t11=['\theta_1=', num2str(t1)];
27 t22=['\theta_2=', num2str(t2)]; t33=['\theta_3=0:2pi'];
28 m11=['m_1=', num2str(m)];
29 info=[pee t11 t22 t33 m11];
30
31 hold on
32
33
34 subplot(2,1,2)
35 plot([0:pas:2*pi], banda1pos)
36 title('Positive_First_Band')
37 xlabel(info)
38 ylabel('Amplitude_[V]')
39 xlim([0 2*pi])
40 grid on
41 grid minor
42 set(gca, 'xtick', [0:pi/2:2*pi])
43 set(gca, 'ytick', [0:0.01:10])
44 set(gca, 'TickLabelInterpreter', 'latex');
45 set(gca, 'XTickLabel', {'0', '$\frac{\pi}{2}$', '$\pi$', '$\frac{3\pi}{2}$', '$2\pi$'})
46 Legend=cell(3,1);
47 Legend{1}='\phi=30  ';
48 Legend{2}='\phi=90  ';
49 Legend{3}='\phi=150  ';
50 legend(Legend)
51
52 hold on
53
54 subplot(2,1,1)
55 plot([0:pas:2*pi], banda1neg)
56 title('Negative_First_Band')
57 xlabel('\theta_3')
58 ylabel('Amplitude_[V]')
59 xlim([0 2*pi])
60 grid on
61 grid minor
62 set(gca, 'xtick', [0:pi/2:100])
63 set(gca, 'ytick', [0:0.01:100])

```

```
64 set(gca, 'TickLabelInterpreter', 'latex');
65 set(gca, 'XTickLabel', {'0', '$$\frac{\pi}{2}$$', '$$\pi$$', '$$\frac{3\pi}{2}$$', '$$2\pi$$'})
66 Legend=cell(3,1);
67 Legend{1}='\phi=30  ' ;
68 Legend{2}='\phi=90  ' ;
69 Legend{3}='\phi=150  ' ;
70 legend(Legend)
71
72 hold on
73
74 banda1neg=[]; banda1pos=[]; banda0=[];
75 end
```

Appendix 6: VPIphotonics Design Suite

As it has already been stated in the paper, the software used for the simulations is VPIphotonics.

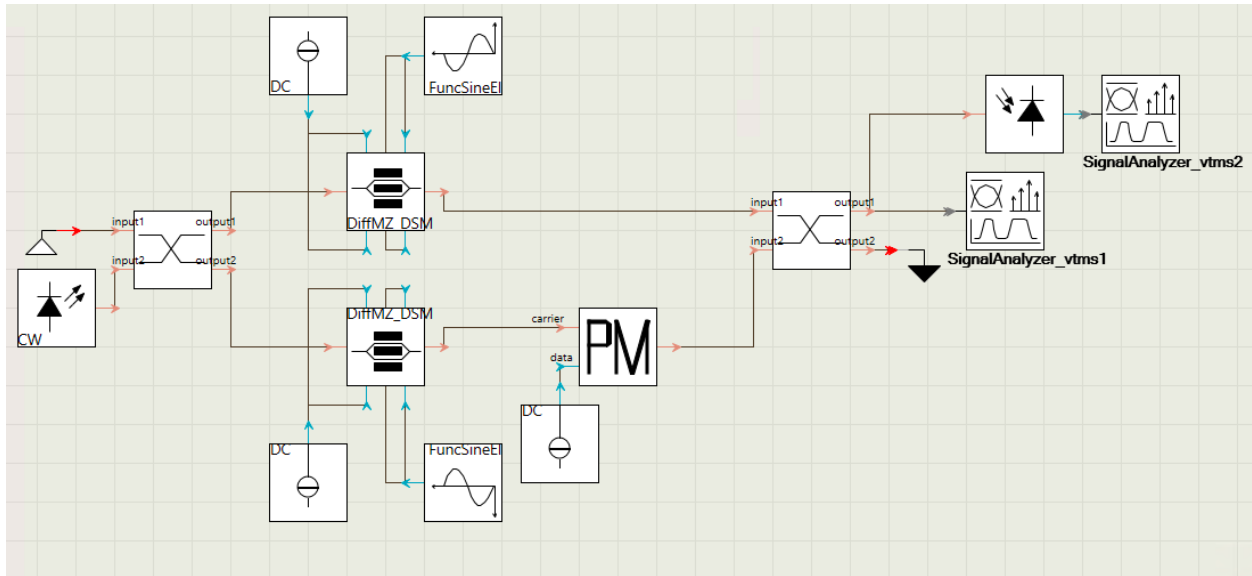


Figura 1: Screenshot of the program used

As seen in the above picture, in each MZM there is a source of V_{bias} and a source of small signal. Also, the input light beam coming from the diode and the signal analyser in the end (the signal analyser connected to the diode on the right obtains the electrical spectrum). The variables that have been changed for the different cases are the amplitudes of both the small and bias signal in the two small MZM, the phase in the second one (ϕ), and the phase difference between the two branches (θ_3).

Other parameters that are constant in all the simulations are:

- RF FREQUENCY: Set to 1 GHz.
- TIME WINDOW: Interval of time where the samples will be considered. $TW = n_r/f_{RF}$, where n_r is a power of two.
- SAMPLE RATIO: Number of samples taken per second. $SR = n_h f_{RF}$, where n_h is the number of harmonics, a power of two.
- EXTINTION RATIO: This parameter is fixed because varying the ER of one of the branches would be easy, but doing it with both of them would be too complex. Since varying only one doesn't make sense, it has been set to the average value of 30.